DALTON
FULL PAPER

New dioxocyclam ligands appended with 2-pyridylmethyl pendant(s): synthesis, properties and crystal structure of their copper(II) complexes (dioxocyclam = 1,4,8,11-tetraazacyclotetradecane-12,14-dione)‡

Xian He Bu,*,†,[a] Dao Li An,[a] Xi Chuan Cao,[a] Ruo Hua Zhang,[a] Thomas Clifford[b] and Eiichi Kimura[b]

[a] *Department of Chemistry, Nankai University, Tianjin 300071, P. R. China*
[b] *Department of Medicinal Chemistry, School of Medicine, Hiroshima University, Kasumi 1-2-3, Minami-Ku, Hiroshima 734, Japan*

Two new dioxocyclam ligands, 4-(pyridin-2-ylmethyl)-1,4,8,11-tetraazacyclotetradecane-12,14-dione (L^1) and 4,8-bis(pyridin-2-ylmethyl)-1,4,8,11-tetraazacyclotetradecane-12,14-dione (L^2), have been synthesized and characterized. The solution chemistry of the Cu^{II} complexes with these ligands have been studied by potentiometric and spectroscopic titration, cyclic voltammetry (CV), UV/VIS and ESR spectral techniques. The Cu^{II} complex of L^2 has been isolated as single crystals and the structure has been determined by X-ray diffraction analysis to be $[CuL^2][ClO_4]_2$ **1**. In complex **1**, the Cu^{II} atom is five-co-ordinate with the two pendant pyridyl nitrogens and the two tertiary amines forming a distorted trigonal-bipyramidal configuration in which the backbone oxygen O(2) co-ordinates to Cu^{II} while the two amido nitrogen groups remained non-deprotonated and non-co-ordinated. To our knowledge, this is the first example of Cu^{II} complexes of dioxotetraamines in which the backbone oxygen co-ordinates to the central metal by twisting the backbone.

The chemistry of macrocyclic dioxotetraamines has received much attention and has been extensively studied in recent years.[1–6] Typically, the 14-membered tetraamine macrocycles cyclam, monooxocyclam, and dioxocyclam (see below), like porphyrins and corrin, incorporate metal ions into their cavities to form stable complexes. Macrocyclic dioxotetraamines are unique chelators for some transition-metal ions. They bear dual structural features of macrocyclic tetraamines and oligopeptides and have many interesting properties and important functions. They can stabilize the higher oxidation states of some transition metals.[1,2a,7,8] These properties have been applied to superoxide dismutase-like catalysts.

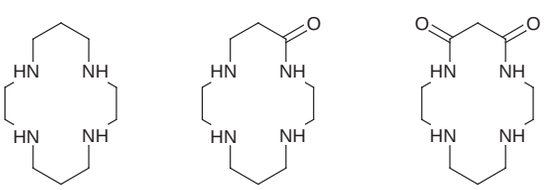

cyclam monooxocyclam dioxocyclam

The two amido groups in macrocyclic dioxotetraamines are equivalent, when co-ordinated to a 3d metal ion, they will be deprotonated simultaneously. As for dioxotetraamine, the presence of a non-deprotonated or a singly deprotonated complex is unlikely, therefore, complexes with this kind of ligand containing non-deprotonated amido groups were generally not considered in previous studies.

So far, great effort has been devoted to the incorporation of functionalized pendant groups into a saturated macrocyclic tetraamine structure (*e.g.* cyclam) to modify its conformational and the redox properties of the metal complex.[9] However, up to now, only a few examples of the macrocyclic dioxotetraamines bearing functionalized pendant groups have been reported.[2i,j,6,10,11] Herein, we report the synthesis and characterization of two novel macrocyclic dioxocyclam (dioxocyclam = 1,4,8,11-tetraazacyclotetradecane-12,14-dione) ligands bearing 2-pyridylmethyl as additional co-ordinating donor pendant(s) (see below), and their complexation properties with Cu^{II} as well as the crystal structure of one of their Cu^{II} complexes. In this complex, the two amido groups remain non-deprotonated, and the backbone oxygen atom co-ordinates to the central Cu^{II} ion by twisting the macrocycle backbone. To our knowledge, this is the first example for the dioxotetraamine metal complexes bearing such features.

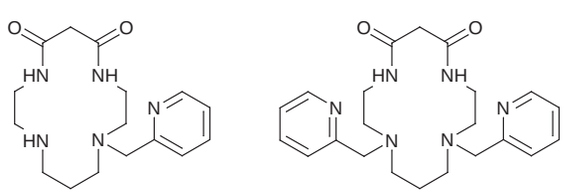

L^1 L^2

Experimental

Materials and methods

Most of the starting materials and solvents for syntheses were obtained commercially and purified prior to use. Dioxocyclam (L^0, 1,4,8,11-tetraazacyclotetradecane-12,14-dione) was prepared according to the literature method.[12] 2-Chloromethylpyridine hydrochloride was purchased from Aldrich and used without further purification. Fourier-transform IR spectra were recorded on a 170SX (Nicolet) spectrometer; EI-MS was carried out on a VG ZAB-HS instrument. Elemental analyses were taken on a P-E 240C analyzer. Proton NMR spectra were recorded on a Bruker AC-P 200 spectrometer (200 MHz) at 25 °C, in $CDCl_3$, with tetramethylsilane as the internal reference. The ESR spectra were measured on a Bruker ER-200-D-SRC10 spectrophotometer. Methanol solutions of copper(II)

† E-Mail: buxh@public1.tpt.tj.cn
‡ *Non-SI unit employed*: G = 10^{-4} T.

complexes [prepared by mixing equimolar amounts of the ligand and $Cu(NO_3)_2$ in methanol solution, and the pH value was adjusted to ≈7 by methanolic NaOH solution] at room temperature and 112 K were used for the measurements. Cyclic voltammetric measurements were performed with a PARC Model 273 electrochemical apparatus in aqueous solution at 25 °C with 0.5 M Na_2SO_4 as supporting electrolyte and pure Ar gas was bubbled through the solution. The concentration of the complexes $Cu(H_{-2}L^0)$, $Cu(H_{-2}L^1)$ and $Cu(H_{-2}L^2)$ were kept at 2×10^{-3} M. The pH was adjusted with concentrated NaOH or H_2SO_4 solution. The cyclic voltammograms at a scan rate of 100 mV s^{-1} were evaluated graphically. A three-electrode system was employed: glassy carbon as working electrode, saturated calomel electrode (SCE) as a reference electrode and Pt as a counter electrode.

All solutions for potentiometric titrations were made up with freshly redistilled water stored over nitrogen. High purity potassium nitrate, Cu^{II} salts, and sodium hydroxide were obtained from Aldrich and used without further purification. Standard HCl was obtained from Nacali Tesque. The concentration of copper(II) nitrate stock solution was determined by H_4edta complexometric titration. Carbonate-free stock solutions of NaOH were prepared by dilution of a chilled 10 M stock solution with distilled, boiled water and then standardised potentiometrically by titrating with standard 0.1000 M HCl. A stock solution of HNO_3 was prepared by diluting concentrated HNO_3. All the other reagents for syntheses and analyses were of analytical grade.

Potentiometric data for the determination of protonation and complexation constants were obtained from a Horiba F-16 pH meter equipped with Horiba reference and pH electrodes. Test solutions were thermostatted using a water-jacketed cell connected to an external circulating water bath (Komatsu-Yamato CTE-310 cooling bath). The UV/VIS spectra for spectrophotometric studies were measured at 25.0 °C using a Hitachi U-3500 spectrometer equipped with a thermoelectric cell-temperature controller coupled to a thermostatted circulating water bath as a secondary heat buffer (0.01).

All measurements were conducted in aqueous solution at 25.0 °C. The electrode was calibrated by titration of standard base against standard acid as described earlier,[13] defining pH as p[H] ($pK_w = -13.79$), and the slope and offset of the electrode calculated from the theoretical concentration of H^+ at a single acidic and a single basic point. The linearity of electrode response and carbonate contamination of the standard NaOH solution (0.100 M) was determined by Gran's method and was found to be less than 1%. All samples were kept under an argon atmosphere (supplied through a NaOH solution and distilled water wash-bottle). The solution temperature was maintained at 25.0 ± 0.1 °C and the ionic strength was maintained at 0.10 M with KNO_3. Aqueous solutions (50 cm^3) of the macrocyclic ligands (1×10^{-3} M) in the presence or absence of Cu^{II} (3×10^{-3} to 8×10^{-4} M) were titrated with standard NaOH solution. Protonation constants were determined from a total of four curves (164 points) for L^1 and three curves (131 points) for L^2. Copper complexation constants were determined from three curves (104 points) for L^1 and two curves (49 points) for L^2.

Syntheses

4-(Pyridin-2-ylmethyl)-1,4,8,11-tetraazacyclotetradecane-12,14-dione (L^1) and 4,8-bis(pyridin-2-ylmethyl)-1,4,8,11-tetraazacyclotetradecane-12,14-dione (L^2). To a solution of 2-chloromethylpyridine hydrochloride (410 mg, 2.5 mmol) in 30 mL of deoxygenated dimethylformamide (DMF) was added dropwise to a solution of dioxocyclam (2.3 g, 10 mmol) in 80 mL of deoxygenated DMF in the presence of excess amount of fine and dried K_2CO_3 at *ca.* 80 °C. The resulting reaction mixture was heated and stirred at 80 °C for about 10 h under Ar. After filtration of the reaction mixture, the filtrate was evaporated to dryness and then dissolved in H_2O and then extracted with $CHCl_3$. The combined $CHCl_3$ solutions were dried and evaporated, and then the residue was purified by column chromatography on silica gel by eluting with CH_2Cl_2–MeOH (100 : 5). The product L^1 was finally recrystallized from acetonitrile as colourless needles (320 mg, 40% based on 2-chloromethylpyridine hydrochloride). ^{1}H NMR ($CDCl_3$): δ ≈1.75 (2 H, m), 2.44–2.67 (8 H, m), 3.26 (2 H, s), 3.32 (2 H, qnt), 3.55 (2 H, qnt), 4.17 (2 H, s), 7.26–7.31 (2 H, m), 7.68–7.69 (2 H, m), 8.52–8.55 (1 H, m). IR (KBr pellet): 546w, 666w, 709w, 760m, 956w, 1043w, 1148m, 1309m, 1357m, 1431m, 1553s, 1629s, 1672s, 2795w, 2800m, 2933m, 3055w, 3325s cm^{-1}. EI-MS: M^+ peak $m/z = 319$ ($M_r = 319.41$) (Found: C, 60.03; H, 8.16; N, 21.90. Calc. for $C_{16}H_{25}N_5O_2$: C, 60.17; H, 7.89; N, 21.93%).

For the preparation of L^2, a solution of 2-chloromethylpyridine hydrochloride (1.64 g, 10 mmol) in 50 mL of deoxygenated DMF was added dropwise to a solution of dioxocyclam (0.760 g, 3.33 mmol) in 50 mL of deoxygenated DMF in the presence of an excess of fine and dried K_2CO_3 at *ca.* 80 °C. The resulting mixture was heated and stirred at *ca.* 80 °C for about 10 h under Ar. After filtration of the reaction mixture, the filtrate was evaporated to dryness and then dissolved in H_2O and then extracted with $CHCl_3$. The combined $CHCl_3$ solutions were dried and evaporated, and then, the residue was purified by column chromatography on silica gel by eluting with CH_2Cl_2–MeOH (100 : 3). The product was finally recrystallized from acetonitrile as colourless needles (0.96 g, 70% based on dioxocyclam). ^{1}H NMR ($CDCl_3$): δ ≈1.75 (2 H, m), 2.44–2.83 (8 H, m), 3.26 (2 H, s), 3.32–3.35 (4 H, m), 3.69 (2 H, s), 7.19–7.28 (4 H, m), 7.62–7.65 (2 H, m), 8.50–8.52 (2 H, m). IR (KBr pellet): 565w, 612w, 727w, 766m, 956w, 1049w, 1160m, 1316m, 1359m, 1433m, 1476w, 1518s, 1567m, 1641s, 1662s, 2801s, 2927m, 3063w, 3307s cm^{-1}. EI-MS: M^+ peak $m/z = 410$ ($M_r = 410.52$) (Found: C, 64.25; H, 7.26; N, 20.23. Calc. for $C_{22}H_{30}N_6O_2$: C, 64.37; H, 7.37; N, 20.47%).

$[CuL^2][ClO_4]_2$ 1. For complex **1** the single crystal suitable for X-ray analysis was obtained by mixing a 1 : 1 molar ratio of $Cu(ClO_4)_2$ and L^2 in deoxygenated MeOH under reflux for *ca.* 15 min. The blue reaction mixture was then filtered. The crystal suitable for X-ray analysis was obtained upon slow evaporation of the solvent (Found: C, 39.51; H, 4.28; N, 12.22. Calc. for $C_{22}H_{30}Cl_2CuN_6O_{10}$: C, 39.27; H, 4.49; N, 12.49%). IR (KBr pellet): 582w, 623m, 768w, 1068s, 1102vs, 1301w, 1446m, 1536w, 1573m, 1631s, 1695s, 2935w, 3125w, 3338s, 3430s (br) cm^{-1}.

Crystallography

A blue crystal (approximately 0.1 × 0.3 × 0.5 mm) of complex **1** was mounted on an Enraf-Nonius CAD-4 diffractometer equipped with a graphite-crystal monochromator situated in the incident beam for data collection. The determination of unit cells and the data collection were performed with Mo-Kα radiation (λ = 0.710 73 Å). Unit-cell dimensions were obtained by least-squares refinements using 25 reflections in the θ range 7.92–13.45°. The intensities of reflections were measured in the ω–2θ scan mode in the range $2 \leqslant \theta \leqslant 23°$ at room temperature (299 ± 1 K). Crystal and instrument stabilities were monitored with a set of three standard reflections measured every 60 min, in all cases no significant variations were found. A total of 4035 reflections were collected and among them 3187 reflections are independent reflections, in which 2031 reflections with $I > 2\sigma(I)$ were considered to be observed and used in the succeeding refinements. The structure was solved by direct methods. All calculations were performed on an IBM 486 personal computer with the Siemens SHELXTL PC program package.[14] The Cu atom was located from an *E*-map. The other non-hydrogen atoms were determined with successive Fourier difference syntheses. The final refinement was done by full-matrix least-

squares methods with anisotropic thermal parameters for non-hydrogen atoms. The refinement agreement factors are $R = 0.064$ and $R' = 0.056$ $\{w = 1/[\sigma^2(F) + 0.0001F^2]\}$. The highest peak and hole on the final Fourier-difference map had a height of 0.75 and -0.68 e Å^{-3}, respectively. The hydrogen atoms were added theoretically, riding on the atoms concerned and refined with fixed thermal factors.

We should note that the crystal was of poor quality even though several attempts were made in different conditions to improve the quality.

Crystal data for complex **1**: $C_{22}H_{30}Cl_2CuN_6O_{10}$, $M = 672.96$, monoclinic, space group $P2_1/c$, $a = 8.962(2)$, $b = 12.588(3)$, $c = 23.940(5)$ Å, $\beta = 92.50°$, $U = 2698.2(1.9)$ Å^3, $D_c = 1.657$ g cm^{-3}, $Z = 4$, $F(000) = 1388$, $\mu = 10.75$ cm^{-1}.

CCDC reference number 186/989.

Results and Discussion

Synthesis of ligands and complexes

The compound dioxocyclam was synthesized following the method reported by Tabushi *et al.*[12] The new ligands were prepared according to Scheme 1. An excessive amount of dioxocyclam (L^0) was used to obtain the monoalkylated product L^1 which was purified by silica gel column chromatography and recrystallized from CH_2Cl_2–MeCN as colourless needles in 40% yield. The doubly-substituted ligand L^2 was also obtained as a by-product and can be isolated by column chromatography from the monoalkylated product. The doubly-substituted product L^2 can be prepared using an excessive amount of 2-chloromethylpyridine hydrochloride. The yield of L^2 in this reaction was 70%. All the analytical and spectral data are in good agreement with the theoretical requirements of the new ligands.

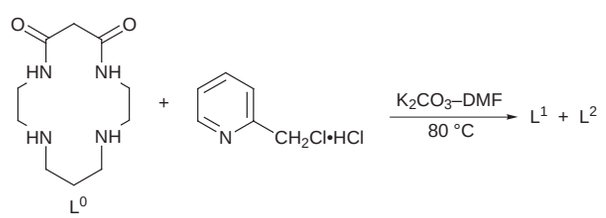

Scheme 1

The new ligand L^2 was treated with 1 equivalent of $Cu(ClO_4)_2$ in deoxygenated MeOH under reflux. The 1 : 1 pyridyl-pendant dioxocyclam–Cu^{II} complex was obtained as blue crystals. The results of elemental analysis (C, H, N) indicated a possible formula of $[CuL^2][ClO_4]_2$. The co-ordination of one of the backbone oxygen atoms and the non-bonding of the amide nitrogens was also confirmed by the IR spectra of the complex [$\nu_{C=O}$: 1631 cm^{-1} for C=O(Cu) and 1695 cm^{-1} for non-co-ordinated C=O]. The non-deprotonated pyridyl-pendant dioxocyclam–Cu^{II} complex is air-stable in the solid state.

Protonation and complexation

Potentiometric titrations. Potentiometric pH measurements and computation of the protonation constants and Cu^{II} binding constants were carried out by procedures described previously.[13] Approximately 1 : 1 L : Cu molar ratios were used. The found/expected error, σ, was found to be less than 12 in all calculations (more than one curve was used in each calculation). The titration curve for L^1 in the presence of 3 equivalents of HNO_3 with standard acid with and without Cu^{II} are shown in Fig. 1 and the corresponding titrations with L^2 are plotted in Fig. 2. The ligands show titratable protons resulting from deprotonation at the pyridyl nitrogens and the amine ring nitrogens but the amide protons are too basic to be deprotonated. The final deprotonation of the L^2 macrocycle occurs at substantially lower pH than for L^1 as this is a deprotonation from a tertiary amine rather than the secondary amine in L^1.

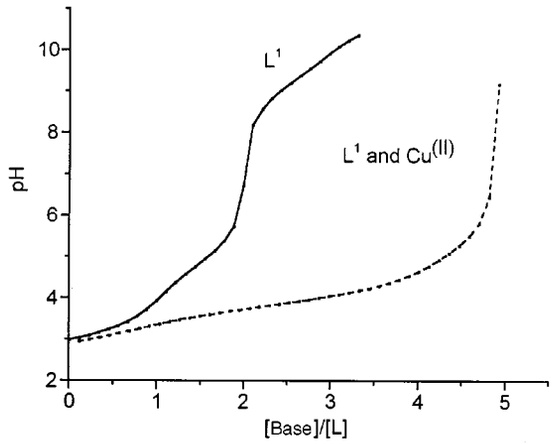

Fig. 1 Titration of L^1 (1×10^{-3} M) with and without addition of Cu^{II} (3×10^{-3} to 8×10^{-4} M) with standard NaOH (0.100 M)

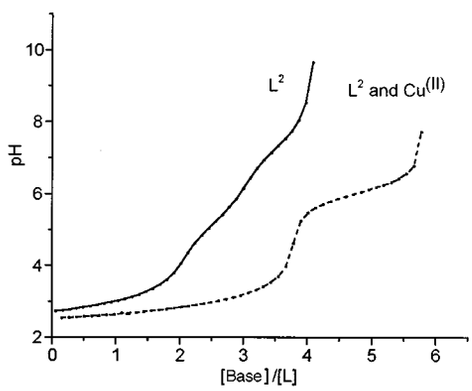

Fig. 2 Titration of L^2 (1×10^{-3} M) with and without addition of Cu^{II} (3×10^{-3} to 8×10^{-4} M) with standard NaOH (0.100 M)

The difference in co-ordinating properties between L^1 and L^2 are evident in the titrations in the presence of Cu^{II}. Ligand L^1 shows only one sharp inflexion point and one buffer region but L^2 has two inflexion points and two buffer regions. The first acidic buffer region in L^2 extends up to an inflexion point at 4 equivalents of base and then a more basic buffer region from 4 to 6 equivalents results from the deprotonation of the amide moieties. The first buffer region indicates the formation of a stable complex of L^2 with the amide groups remaining protonated which is quite unusual for a macrocyclic amide.

Presumably the ligand can co-ordinate through the pyridyl sidearms and the two ring amines to form a stable Cu^{II} complex. The structure of this species was investigated further in the spectrophotometric study below. Processing of the titration data in HYPERQUAD[15] revealed the presence of a minor monodeprotonated L^2 complex as well as the dideprotonated L^2–Cu^{II} complex as the major species at high pH. Ligand L^1 shows a rather different species composition and distribution. The monodeprotonated Cu^{II} complex of L^1 was a more important species and there was no neutral L^1 complex although there was a protonated Cu^{II} complex. This will be due to the rather weaker complexing ability with only one pyridine side arm. The single armed macrocycle is unable to stabilize a neutral ligand complex with Cu^{II} outside the macrocyclic ring. However at low enough pH protonation of the ring enables Cu^{II} to be bound outside the ring through the pyridyl and one ring amine. At higher pH the metal pops into the ring with concomitant deprotonation of the macrocyclic amides.

Table 1 Potentiometrically determined equilibrium constants for the reaction of L^1 or L^2 with Cu^{II} and hydrogen ion *

Reaction	Equilibrium quotient, K	log K
$L^1 + H \rightleftharpoons L^1H$	$[L^1H]/[L^1][H]$	9.154(2)
$L^1H + H \rightleftharpoons L^1H_2$	$[L^1H^2]/[L^1H][H]$	13.978(3)
$Cu + L^1 \rightleftharpoons CuH_{-1}L^1 + H$	$[CuH_{-1}L^1][H]/[Cu][L^1]$	5.77(2)
$Cu + L^1 \rightleftharpoons CuH_{-2}L^1 + 2H$	$[CuH_{-2}L^1][H]^2/[Cu][L^1]$	0.64(2)
$L^2 + H \rightleftharpoons L^2H$	$[L^2H]/[L^2][H]$	7.190(7)
$L^2H + H \rightleftharpoons L^2H_2$	$[L^2H_2]/[L^2H][H]$	5.12(1)
$L^2H_2 + H \rightleftharpoons L^2H_3$	$[L^2H_3]/[L^2H_2][H]$	1.86(5)
$Cu + L^2 \rightleftharpoons CuL^2$	$[CuL^2]/[Cu][L^2]$	11.10(2)
$CuL^2 \rightleftharpoons CuH_{-1}L^2 + H$	$[CuH_{-1}L^2][H]/[CuL^2]$	−6.38(4)
$CuL^2 \rightleftharpoons CuH_{-2}L^2 + 2H$	$[CuH_{-2}L^2][H]^2/[CuL^2]$	−12.03(3)
$OH_2 \rightleftharpoons H + OH$	$[OH][H]/[OH_2]$	−13.79

* Charges omitted for clarity.

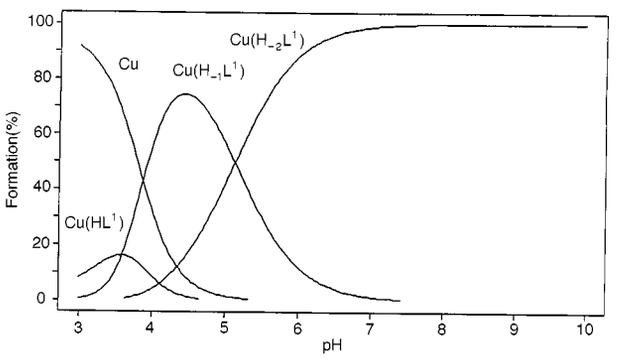

Fig. 3 Speciation curves of the complexes of L^1 in the presence of 1 equivalent of Cu^{II}

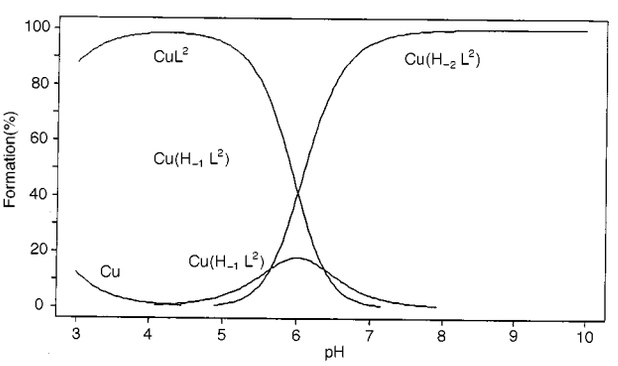

Fig. 4 Speciation curves of the complexes of L^2 in the presence of 2 equivalents of Cu^{II}

The equilibria are collected in Table 1 and the calculated species distribution diagrams for the Cu^{II} complexes of L^1 and L^2 are shown in Figs. 3 and 4, respectively.

Spectrophotometric titration. The rather unusual co-ordinating behaviour of L^2 with Cu^{II} prompted us to make a spectrophotometric study from which we could propose structures for the species identified in the potentiometric study. Under approximately the same conditions as for the potentiometric titrations, a visible spectrum (wavelength range 850–400 nm) was taken after each aliquot of standard sodium hydroxide was added. The absorbances were converted to molar extinctions and plotted out in Fig. 5. Unfortunately the changes in the absorbances were either insufficiently large or the accuracy of the absorbance measurements were not good enough to make a full HYPERQUAD calculation on the data, however, input of the potentiometrically determined equilibrium constants as a model for the solution chemistry allowed us to deconvolute the spectra in HYDRASP, a sub-program of HYPERQUAD,[15] to give molar absorbances of the four absorbing species in

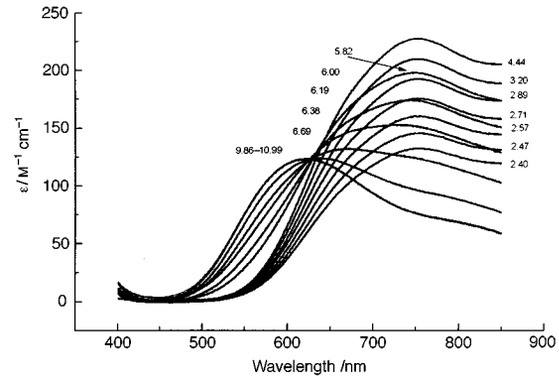

Fig. 5 Absorption coefficient *vs.* wavelength for spectra taken over the course of a titration of L^2 in the presence of Cu^{II} with standard NaOH

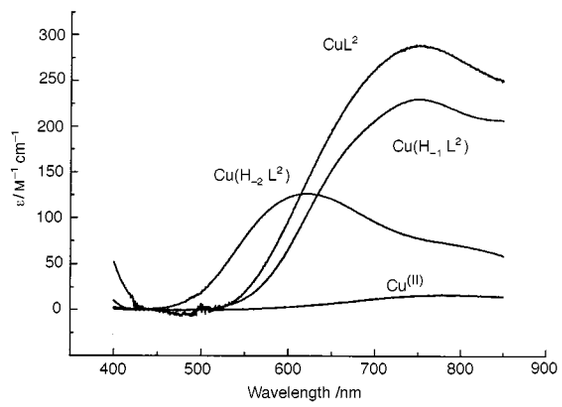

Fig. 6 Calculation of absorption coefficients of individual Cu^{II} complex species of L^2

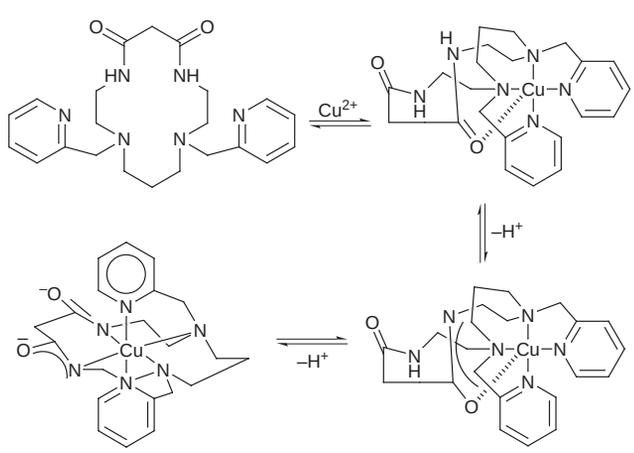

Fig. 7 Proposed structures of CuL^2, $Cu(H_{-1}L^2)$ and $Cu(H_{-2}L^2)$

solution. A graph of molar absorbances *vs.* wavelength for the absorbing species is shown in Fig. 6. The graph shows more clearly what can be inferred by inspection of the spectra in Fig. 5.

The deprotonation of the amides result in a blue shift of the spectrum as the ligand field is increased. What is interesting however is the similarity of the molar absorbances of the neutral ligand complex and that for the monodeprotonated amide complex. This suggests a similarity of co-ordination geometry of the two species and indicates that Cu^{II} is also located outside the macrocyclic cavity in the monodeprotonated amide macrocycle as well. Possibly the neutral and monodeprotonated L^2–Cu^{II} complexes have the structure given in Fig. 7, where Cu^{II} is in a distorted trigonal bipyramidal co-ordination environment chelated by the pyridyl sidearms, the macrocycle ring amines and the oxygen of one of the amide moieties. A deprotonation of the second amide results in the metal entering the ring to

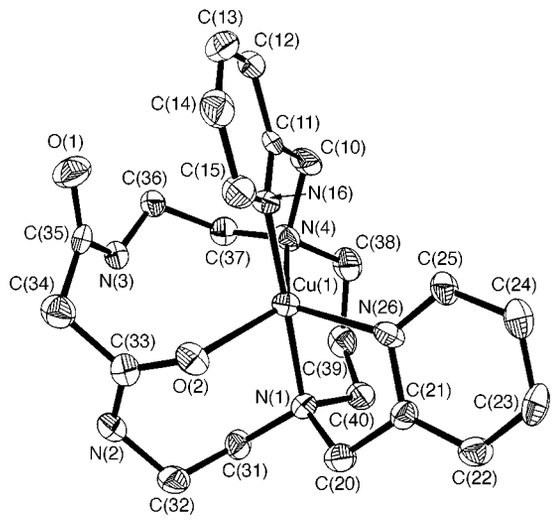

Fig. 8 The ORTEP[16] drawing of complex **1** with 35% probability thermal ellipsoids

Table 2 Selected bond lengths (Å) and bond angles (°) for complex **1** with estimated standard deviations in parentheses

Cu(1)–O(2)	2.092(6)	Cu(1)–N(1)	2.014(6)
Cu(1)–N(4)	2.127(6)	Cu(1)–N(16)	1.971(6)
Cu(1)–N(26)	2.061(7)	O(1)–C(35)	1.215(10)
O(2)–C(33)	1.246(10)	N(1)–C(20)	1.484(10)
N(1)–C(31)	1.518(11)	N(1)–C(40)	1.505(11)
N(2)–C(32)	1.453(11)	N(2)–C(33)	1.309(10)
N(3)–C(35)	1.343(11)	N(3)–C(36)	1.453(10)
O(2)–Cu(1)–N(1)	86.6(2)	O(2)–Cu(1)–C(4)	133.9(2)
O(2)–Cu(1)–N(16)	90.5(3)	O(2)–Cu(1)–C(26)	101.9(2)
N(1)–Cu(1)–N(4)	100.8(3)	N(1)–Cu(1)–C(16)	176.2(3)
N(1)–Cu(1)–N(26)	82.4(3)	N(4)–Cu(1)–C(26)	124.1(3)
N(4)–Cu(1)–N(16)	82.9(3)	N(16)–Cu(1)–N(26)	95.9(3)
Cu(1)–N(1)–C(20)	104.6(5)	Cu(1)–N(1)–C(40)	109.2(5)
C(31)–N(1)–C(40)	106.4(6)	C(32)–N(2)–C(33)	121.2(7)
C(35)–N(3)–C(36)	125.2(7)	Cu(1)–N(4)–C(10)	103.1(5)
Cu(1)–N(16)–C(15)	123.0(5)	Cu(1)–N(26)–C(21)	110.8(5)
Cu(1)–N(26)–C(25)	130.7(5)	O(2)–C(33)–C(34)	119.7(7)

form the macrocyclic complex resulting in a strongly blue-shifted spectrum commonly found with macrocyclic amides.

Description of crystal structure

The molecular structure of complex **1** is shown in Fig. 8. The important bond lengths and angles are listed in Table 2. From Fig. 8, it is obvious that in complex **1**, the Cu atom is five-co-ordinate with O(2), N(1), N(4), N(16), N(26) and forms a distorted trigonal-bipyramidal configuration. The two amide nitrogens [N(2), N(3)], remained nondeprotonated and do not take part in the co-ordination with Cu^{II}. The Cu(1)–N(4) bond distance of 2.127(6) Å, is the longest one among the co-ordination bonds indicating weaker co-ordination due to Jahn–Teller effects. The Cu^{II} ion is nearly in the plane formed by O(2), N(4), N(26). One of the oxygen atoms in the dioxocyclam backbone [O(2)] co-ordinates to Cu(1). This may be the first example of Cu^{II} complexes of macrocyclic dioxotetraamines in which a backbone oxygen co-ordinates to the central metal ion by twisting the backbone.

The distances of N(2)–C(33) [1.309(10) Å] and N(3)–C(35) [1.343(11) Å] are obviously shorter than a normal C–N distance (1.47 Å) and show partial double bond character which may arise from the conjugation between O(2)–C(33)–N(2) and O(1)–C(35)–N(3). The dihedral angle between the pyridine pendants is 71.4°, which means that two pyridine pendants are in close proximity perpendicularly to each other when co-ordinating to Cu^{II}. The dihedral angle between O(2)–N(4)–N(26) and the co-ordinated pyridine plane N(16)–C(11)–C(15) is 98.96°, the other dihedral angle between O(2)–N(4)–N(26) and N(26)–C(21)–C(25) is 66.00°. In the unit cell of complex **1**, a perchlorate ion links with the macrocycle of the complex through hydrogen bonding.

Table 3 Electrochemical data of the Cu^{II} complexes of L^0 and L^1 *

Ligand	L^0	L^1
pH	≈5.5	≈6
E_{pa}/V	0.58	0.77
E_{pc}/V	0.71	0.88
ΔE_p/mV	130	90
$E_{\frac{1}{2}}$/V	0.64	0.83

* Cyclic voltammograms in H_2O at 25 °C, in V *vs.* SCE; scan rate 100 mV s^{-1}. The concentration of the complexes of L^0 and L^1 were kept at 2×10^{-3} M. Reversible redox voltammograms have not been obtained for Cu^{II}–L^2 complexes.

Electrochemical studies

The cyclic voltammograms of the Cu^{II} complexes of L^0 and L^1 were examined in aqueous solution (0.5 M Na_2SO_4) at 25 °C, and the electrochemical data are summarized in Table 3. The cyclic voltammograms showed one quasi-reversible oxidation wave. The $Cu^{III/II}$ potential of $Cu(H_{-2}L^1)$, +0.83 V *vs.* SCE, is 0.19 V more positive than that for $Cu(H_{-2}L^0)$ under similar conditions ($E_{\frac{1}{2}} = 0.64$ V *vs.* SCE),[1a] implying that the ligand L appended with 2-pyridylmethyl destabilizes the Cu^{III} state compared with the unsubstituted L^0.

This behaviour can be interpreted as follows: the change from Cu^{II} state (d^9) to Cu^{III} state (d^8, low spin) involves a drastic reduction of the metal ion radius and a change of electronic configuration (Scheme 2).[6] In the new complex, the pyridine

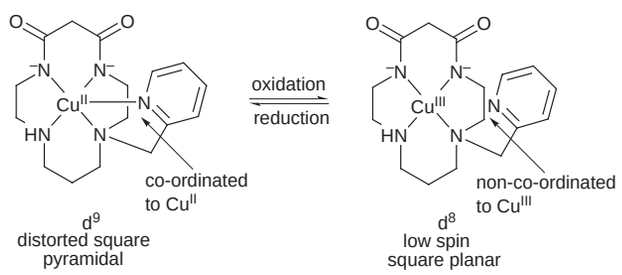

Scheme 2

pendant co-ordinates to the central Cu^{II} from the apical site, and the Cu^{II} ion resides above the mean plane of the four basal nitrogens. The co-ordination of one pyridine pendant to Cu^{II} stabilizes the Cu^{II} ion. But when Cu^{II} is oxidized to Cu^{III}, like Ni^{II} (d^8, low spin), Cu^{III} tends to adopt a square-planar co-ordination rather than a five-co-ordinate one, which means the pyridine pendant will not co-ordinate to Cu^{III}. Since N-substitution by the pyridine pendant(s) increases the steric constraint of the macrocyclic ring and lowers the co-ordinative ability of the macrocycle, the Cu^{III} ion in the new ligands are not stabilized to the same extent as in the unsubstituted dioxocyclam. The results are similar to that of the Cu^{II} complex of dioxocyclam appended with 8-methylquinoline.[11]

ESR Studies

Fig. 9 represents the ESR spectra of $Cu(H_{-2}L^1)$ in MeOH solution at room temperature and 112 K in higher pH regions (in this region the doubly-deprotonated Cu^{II} complexes are formed). For complex $Cu(H_{-2}L^1)$, it can be seen that the spectrum of the complex is split into four equally spaced absorptions by the interaction with the Cu^{II} nucleus ($I = \frac{3}{2}$) [Fig. 9(a)]

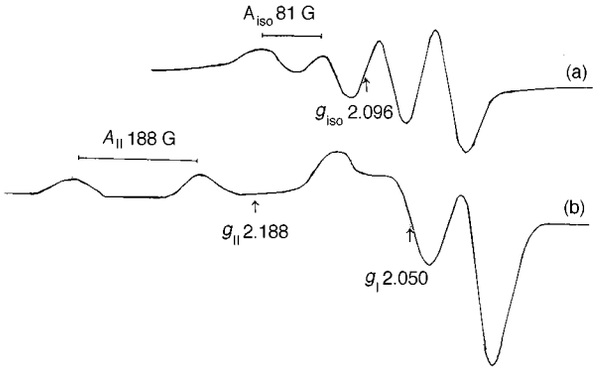

Fig. 9 The X-band ESR spectra of complex $Cu(H_{-2}L^1)$ in MeOH at (a) 298 K, and (b) 112 K

Table 4 The ESR parameters of the Cu^{II} complexes of L^0, L^1 and L^2 in methanol solution at room temperature and 112 K *

	298 K		112 K			
Ligand	g_{iso}	A_{iso}/G (10^3 cm^{-1})	$g_{\|}$	$g_{\perp}$	$A_{\|}$/G (10^2 cm^{-1})	$A_{\perp}$/G (10^3 cm^{-1})
L^0	2.086	96 (9.41)	2.173	2.043	208 (2.124)	40 (3.84)
L^1	2.096	81 (7.98)	2.188	2.050	188 (1.933)	28 (2.70)
L^2	2.103	72 (7.12)	2.194	2.058	184 (1.897)	16 (1.65)

* $A_{\perp}$ was calculated according to the formula $3A_{iso} = A_{\|} + 2A_{\perp}$ and $g_{\perp}$ according to the formula $3g_{iso} = g_{\|} + 2g_{\perp}$.

at room temperature. The isotropic ESR parameters are listed in Table 4. When these solutions are frozen at 112 K, ESR spectra characteristic of nearly axial symmetry are observed, which are very similar to that of $Cu(H_{-2}L^0)$ and $Cu(H_{-2}L^2)$ complexes. The approximate ESR parameters of complex $Cu(H_{-2}L^1)$ are graphically evaluated as $g_{\|} = 2.188$, $g_{\perp} = 2.050$, $A_{\|} = 188$ G (1.933×10^{-2} cm^{-1}), and $A_{\perp} = 28$ G (2.70×10^{-3} cm^{-1}), where $g_{\perp} = (3g_{iso} - g_{\|})/2$ and $A_{\perp} = (3A_{iso} - A_{\|})/2$.[17] It is obvious that the observed $A_{\|}$ values decrease and $g_{\|}$ values increase from $Cu(H_{-2}L^0)$ to $Cu(H_{-2}L^1)$ and $Cu(H_{-2}L^2)$. The tendencies for $A_{\|}$ to decrease and $g_{\|}$ to increase have been taken as parameters to measure the lowering of the strength of in-plane ligand fields under the tetragonal basal square arrangement of Cu^{II} complexes.[18] Therefore, ESR spectra also support the weakened in-plane bonding in complexes $Cu(H_{-2}L^1)$ and $Cu(H_{-2}L^2)$. This is in consistent with the CV measurements. The ESR parameters of these complexes also indicate a $d_{x^2-y^2}$ ground-state of Cu^{II} in these complexes.

Acknowledgements

We gratefully acknowledge the financial support from the National Natural Science Foundation of China (No. 29771022) and Tianjin Natural Science Foundation, China (to X. H. B.). The ESR spectra and CV were carried out at the National Key Laboratory on Coordination Chemistry in Nanjing University, China.

References

1 (*a*) E. Kimura, *J. Coord. Chem.*, 1986, **15**, 1; (*b*) E. Kimura, *Pure Appl. Chem.*, 1986, **58**, 1461; (*c*) E. Kimura, *Crown Compounds Toward Future Applications*, ed. S. R. Cooper, VCH, New York, 1992, ch. 6.

2 (*a*) M. Kodama and E. Kimura, *J. Chem. Soc., Dalton Trans.*, 1979, 325; (*b*) M. Kodama and E. Kimura, *ibid.*, 1979, 1783; (*c*) M. Kodama and E. Kimura, *ibid.*, 1981, 694; (*d*) K. Ishizu, J. Hirai, M. Kodama and E. Kimura, *Chem. Lett.*, 1979, 1045; (*e*) R. Machida, E. Kimura and M. Kodama, *Inorg. Chem.*, 1983, **22**, 2055; (*f*) E. Kimura, T. Koike, R. Machida, R. Nagai and M. Kodama, *Inorg. Chem.*, 1984, **23**, 4181; (*g*) E. Kimura, C. A. Dalimunte, A. Yamashita and R. Machida, *J. Chem. Soc., Chem. Commun.*, 1985, 1041; (*h*) E. Kimura, Y. Lin, R. Machida and H. Zenda, *ibid.*, 1986, 1020; (*i*) E. Kimura, S. Korenari, M. Shionoya and M. Shiro, *ibid.*, 1988, 1166; (*j*) E. Kimura, M. Shionoya, M. Okamoto and H. Nada, *J. Am. Chem. Soc.*, 1988, **110**, 3679; (*k*) M. Shionoya, E. Kimura and Y. Iitaka, *ibid.*, 1990, **112**, 9237.

3 R. W. Hay, M. P. Pujari and F. McLaren, *Inorg. Chem.*, 1984, **23**, 3033; L. Fabbrizzi, *Inorg. Chem.*, 1985, **4**, 33; L. C. Siegfried and T. A. Kaden, *J. Phys. Org. Chem.*, 1992, 549; L. Fabbrizzi, A. Perotti, A. Profumo and T. Soldi, *Inorg. Chem.*, 1986, **25**, 4256; L. Fabbrizzi, F. Forlini, A. Perotti and B. Seghi, *Inorg. Chem.*, 1984, **23**, 807; L. Fabbrizzi, T. A. Kaden, A. Perotti, B. Seghi and L. Seigfried, *Inorg. Chem.*, 1986, **25**, 321; G. D. Santis, L. Fabbrizzi, M. Licchelli and P. Pallavicini, *Coord. Chem. Rev.*, 1992, **120**, 237.

4 E. Kimura and H. Nada, *Tanpakushitsu Kakusan Koso*, 1988, **16**, 2914; R. Machida, E. Kimura and M. Kodama, *Inorg. Chem.*, 1983, **22**, 2055; E. Kimura and R. Machida, *Yuki Gosei Kagaku Kyokaishi*, 1984, **42**, 407.

5 B. J. Hathaway, in *Comprehensive Coordination Chemistry*, ed. G. Wilkinson, Pergamon Press, Oxford, 1987, **5**, p. 533.

6 X. H. Bu, D. L. An, Y. T. Chen, M. Shionoya and E. Kimura, *J. Chem. Soc., Dalton Trans.*, 1995, 2289; X. H. Bu, X. C. Cao, D. L. An, R. H. Zhang, T. Clifford and E. Kimura, *ibid.*, 1998, 433.

7 L. Fabbrizzi and A. Poggi, *J. Chem. Soc., Chem. Commun.*, 1980, 646; L. Fabbrizzi, A. Perotti and A. Poggi, *Inorg. Chem.*, 1983, **22**, 1411; L. Fabbrizzi, A. Perotti, A. Profumo and T. Soldi, *Inorg. Chem.*, 1986, **25**, 4256; R. Hay, R. Rembi and W. Sommerville, *Inorg. Chim. Acta*, 1982, **59**, 147; Y. D. Lampeka and S. P. Gavrish, *J. Coord. Chem.*, 1990, **21**, 351.

8 D. W. Margerum and G. D. Oven, in *Metal Ions in Biological Systems*, ed. H. Sigel, Marcel Dekker, New York, 1981, vol. 12, p. 75; T. R. Wagner and C. J. Burrows, *Tetrahedron Lett.*, 1988, **29**, 5091; T. R. Wagner, Y. Fang and C. J. Burrows, *J. Org. Chem.*, 1989, **54**, 1584.

9 See, for example, E. Kimura, *J. Inclusion Phenom.*, 1989, **7**, 183; E. Kimura, *Pure Appl. Chem.*, 1989, **61**, 823; E. Kimura, *Tetrahedron*, 1992, **48**, 6175; P. V. Bernhardt and G. A. Lawrence, *Coord. Chem. Rev.*, 1990, **104**, 297; T. A. Kaden, *Crown Compounds Toward Future Applications*, ed. S. R. Cooper, VCH, New York, 1992, ch. 8; E. Kimura, X. H. Bu, M. Shionoya, S. Wada and S. Maruyama, *Inorg. Chem.*, 1992, **31**, 4542; X. H. Bu, Y. T. Chen, M. Shionoya and E. Kimura, *Polyhedron*, 1994, **13**, 325; E. Kimura, S. Wada, M. Shionoya and Y. Okazaki, *Inorg. Chem.*, 1994, **33**, 770.

10 E. Kimura, T. Koike, R. Machida, R. Nagai and M. Kodama, *Inorg. Chem.*, 1984, **23**, 4181; E. Kimura, T. Koike, H. Nada and Y. Iitaka, *ibid.*, 1988, **27**, 1036.

11 X. H. Bu, D. L. An and Y. T. Chen, M. Shionoya, E. Kimura, *J. Inclusion Phenom.*, 1997, **27**, 245.

12 I. Tabushi, H. Okino and Y. Kuroda, *Tetrahedron Lett.*, 1976, 4339.

13 E. Kimura, T. Kioke, K. Uenishi, M. Hedigar, M. Kuramoto, S. Joko, M. Kodama and Y. Iitaka, *Inorg. Chem.*, 1987, **26**, 2975.

14 G. M. Sheldrick, SHELXTL PC, Siemens Analytical X-Ray Instruments, Inc., Madison, WI, 1990.

15 P. Gans, A. Sabatini and A. Vacca, *Talanta*, 1996, **43**, 1739.

16 C. K. Johnson, ORTEP, Report ORNL-5138, Oak Ridge National Laboratory, Oak Ridge, TN, 1976.

17 K. Miyoshi, H. Tanaka, E. Kimura, S. Tsuboyama, S. Murata, H. Shimizu and K. Ishizu, *Inorg. Chim. Acta*, 1983, **78**, 23.

18 A. S. Brill, *Molecular Biology Biochemistry and Biophysics. 26. Transition Metals in Biochemistry*, ed. A. Kleinzeller, Springer-Verlag, New York, 1977, p. 43.

Received 5*th December* 1997, *revised manuscript received* 25*th March* 1998; *Paper* 8/02327A